

Solid-State NMR Study of Titanium Dioxide Nanoparticles Surface-Modified by Alkylphosphonic Acids

Hiroyuki Souma, Ryo Chiba, and Shigenobu Hayashi*

Research Institute of Instrumentation Frontier, National Institute of Advanced Industrial Science and Technology (AIST), Tsukuba Central 5, 1-1-1 Higashi, Tsukuba, Ibaraki 305-8565

Received June 14, 2011; E-mail: hayashi.s@aist.go.jp

We have modified the surface of TiO_2 nanoparticles by propylphosphonic acid (PPA) and decylphosphonic acid (DPA), and have characterized the surface layer of titania (=titanium dioxide) nanoparticles by means of high-resolution solid-state NMR of ^{31}P, ^{1}H, and ^{13}C, X-ray powder diffraction, and themogravimetric analysis. The ^{31}P NMR spectra showed four types of bonding states corresponding to the monodentate and bidentate bonding states. The ^{1}H NMR spectra demonstrated decrease in P–OH groups due to the dehydration condensation reaction. Layered titanium alkylphosphonate was formed by prolonged heating of the mixed solution of the reactants. The layered structure was confirmed by X-ray powder diffraction, and the interlayer distance suggested bilayer arrangement of the *n*-alkyl chains in the interlayer space. The ^{31}P NMR spectra showed that a tridentate bonding state was formed in the layered structure. The ^{13}C NMR results suggested all-*trans* conformation of *n*-alkyl chains, and the methyl group was confined in a small space. The molecular axis of the *n*-alkyl chains was tilted from the perpendicular of the layer plane. The surface coverage of the organic modifier in the modified TiO_2 nanoparticles was estimated from the mass loss of thermogravimetric analysis. The surface coverages are about 50%, except for the samples containing considerable amounts of the layered structure.

Chemical functionalities are introduced on the surface of inorganic substrates by anchoring organic monolayers or self-assembled monolayers (SAMs).[1] Organophosphorus compounds such as alkylphosphonates and phosphonic acids are attracting increasing attention, because they bind strongly on various metal oxides.[2–4] Alkylphosphonates form a hydrophobic layer on titania (=titanium dioxide) and zirconia (=zirconium dioxide).[5] Surface modification of inorganic nanoparticles with organic substances is useful to disperse nanoparticles into an organic medium homogeneously.[6] Aggregation of nanoparticles can be suppressed by surface modification.

Solid-state NMR is a powerful method to characterize the surface layers at atomic and molecular levels. ^{31}P NMR is suitable to characterize the surface binding of alkylphosphonates.[2–4,7] ^{17}O NMR can distinguish between P–OH, P=O, P–O–Ti, and Ti–O–Ti,[8,9] although ^{17}O-enriched samples are necessary. ^{1}H NMR can reveal hydrogen-bonding interactions in the monolayers.[10] Molecular ordering in the monolayer can be characterized by ^{13}C NMR.[2,3,7,11]

In the present work, we have modified the surface of titania nanoparticles by propylphosphonic acid (PPA) and decylphosphonic acid (DPA). We have characterized the surface-modified titania nanoparticles by means of high-resolution solid-state NMR of ^{31}P, ^{1}H, and ^{13}C nuclei as well as X-ray powder diffraction and thermogravimetric analysis. The bonding state of phosphonate groups on the TiO_2 surface was revealed by ^{31}P NMR spectra.

Experimental

Materials. Titanium(IV) oxide nanopowder (TiO_2, anatase, 99.7%) was obtained from Aldrich (USA), whose nominal properties were the particle size of less than 25 nm and the surface area of 200–220 $m^2 g^{-1}$. PPA (CH_3–CH_2–CH_2–$P(O)(OH)_2$, 95%) and DPA (CH_3–$(CH_2)_9$–$P(O)(OH)_2$, 97%) were obtained from Aldrich (USA) and Strem Chemicals (USA), respectively.

The surface-modified samples were prepared according to Gao et al.[3] Typical conditions were as follows: A 5-fold excess of alkylphosphonic acid (PPA or DPA) relative to the amount necessary for a full surface coverage on the particles (assuming an area of 0.24 nm^2 per molecule) was dissolved in 100 mL of a 3:1 methanol–water mixed solvent. To the above solution, a suspension of 0.2 g of TiO_2 nanopowder in 20 mL of deionized water was added dropwise. The resulting suspension was stirred at 373 K for several days. The solid part was separated by centrifugation and washed with 40 mL of methanol to remove unreacted alkylphosphonic acid as well as physisorbed species. The process of centrifugation and washing was recycled seven times. The product was dried under vacuum at room temperature.

Six surface-modified samples were prepared, as listed in Table 1. Three samples used PPA as the modifier, and the remaining samples used DPA. The reaction temperature and time were also listed in the table. The reaction temperature was controlled by an oil bath and a mantle heater, where the magnitudes of the temperature fluctuation were about 1 and 20 K, respectively.

NMR Measurements. ^{31}P, ^{1}H, and ^{13}C magic-angle-spinning (MAS) NMR spectra were measured at room temperature with a Bruker ASX400 spectrometer and a Bruker MSL400 spectrometer at Larmor frequencies of 161.98, 400.13, and 100.61 MHz, respectively. Bruker MAS probe-

Published on the web October 29, 2011; doi:10.1246/bcsj.20110185

Table 1. Surface-Modified Samples and Synthetic Conditions

Sample name	Modifier	Temperature /K	Time /day
PPA/TiO_2-1	PPA	373 ± 20	3
PPA/TiO_2-2	PPA	373 ± 1	1
PPA/TiO_2-3	PPA	373 ± 1	3
DPA/TiO_2-1	DPA	373 ± 20	3
DPA/TiO_2-2	DPA	373 ± 1	1
DPA/TiO_2-3	DPA	373 ± 1	3

heads were used with a zirconia rotor of 4.0-mm outer diameter. The pulse sequences for ^{31}P and ^{13}C measurements were a cross-polarization pulse sequence with high-power ^1H decoupling during signal acquisition (CP). The ordinary single-pulse sequence was used for ^1H measurements. The spin–lattice relaxation time, T_1, of ^{31}P was measured by the Torchia sequence.[12] The frequency scale of the ^{31}P spectrum was expressed with respect to 85% H_3PO_4 aqueous solution by adjusting the signal of $(NH_4)_2HPO_4$ to 1.33 ppm.[13] The ^1H spectrum was expressed with respect to neat tetramethylsilane (TMS) by adjusting the signal of adamantane spinning at 8.0 kHz to 1.87 ppm.[14] The ^{13}C spectrum was expressed with respect to neat tetramethylsilane (TMS) by adjusting the CO signal of glycine to 176.46 ppm.[15] The samples were packed into the 4-mm MAS rotor under N_2 atmosphere in a glove bag.

X-ray Powder Diffraction. X-ray powder diffraction patterns were measured by a Rigaku MiniFlex diffractometer with Cu Kα radiation at room temperature in an air atmosphere. The diffraction angle was scanned from 2 to 30° with a rate of 0.02° min^{-1}.

Thermogravimetric Analysis. Thermogravimetric and differential thermal analyses (TG-DTA) were performed with a Rigaku Thermo Plus TG 8120 under an air flow. The samples were heated up to 1073 K with a heating rate of 5 K min^{-1}.

Results and Discussion

^{31}P MAS NMR. Bonding states of alkylphosphonic acid on TiO_2 surface can be probed by ^{31}P NMR. Figure 1 shows ^{31}P CP/MAS NMR spectra of crystalline PPA and three PPA/TiO_2 samples. Crystalline PPA has a chemical shift of 37.4 ppm. The PPA/TiO_2 samples show overlapping signals that spread between 40 and 10 ppm and a sharp signal at 8.4 ppm. The overlapping signals between 40 and 10 ppm consist of at least four components. A very broad signal is observed around 0 ppm. The spectra are deconvoluted into several components assuming Gaussian or Lorentzian line shapes. The deconvolution results between 40 and 10 ppm are drawn in Figure 1, and the parameters of each component are summarized in Table 2. We used cross polarization (CP) from ^1H to ^{31}P instead of direct polarization of ^{31}P in order to increase the efficiency of the signal accumulation. The ^{31}P spin–lattice relaxation time, T_1, of the 28-ppm signal is 6 s for PPA/TiO_2-1, whereas the ^{31}P T_1 value is 340 s for crystalline PPA. The fractions in Table 2 should be regarded only as a guide, because quantitativeness of the signal intensity is largely distorted by the use of CP.

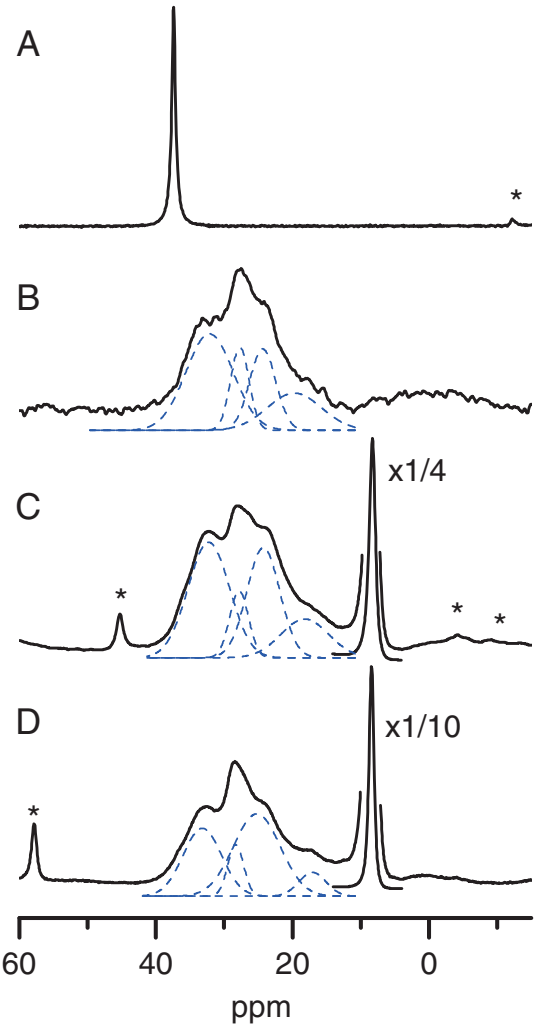

Figure 1. ^{31}P CP/MAS NMR spectra of (A) crystalline PPA, (B) PPA/TiO_2-1, (C) PPA/TiO_2-2, and (D) PPA/TiO_2-3. The spinning rates were (A) 8.07, (B) 8.01, (C) 6.00, and (D) 8.00 kHz. The repetition times were (A) 30 and (B–D) 1 s, and the accumulation numbers were (A) 8, (B) 13616, (C) 8401, and (D) 222246. The mark * indicates spinning sideband. The chain lines show components created by deconvolution in the range between 40 and 10 ppm.

Alkylphosphonic acid reacts with the titania surface by two possible reactions as follows:

$$\text{–P–OH} + \text{HO–Ti} \rightarrow \text{–P–O–Ti} + H_2O \quad (1)$$

$$\text{–P=O} + \text{Ti} \rightarrow \text{–P–O–Ti} \quad (2)$$

Reaction (1) is dehydration condensation reaction, while reaction (2) is addition of –P=O to a Lewis acid site. There are five kinds of bonding states; two monodentate, two bidentate, and one tridentate bonding states, as shown in Figure 2.

Negative frequency shift takes place in the ^{31}P signal when alkylphosphonic acid binds on the surface of titania, zirconia, and silica (=silicon dioxide).[2–4,16,17] The magnitude of the frequency shift suggests the bonding state. In the case of silica, the reaction (1) caused frequency shifts of about −4 and

Table 2. Deconvolution Results of ^{31}P CP/MAS NMR Spectra[a)]

Sample	^{31}P chemical shift/ppm (Fraction/%)					
	I	II	III	IV	V	VI
PPA/TiO_2-1	32.2 (45)	27.7 (15)	24.4 (21)	19.7 (20)		
PPA/TiO_2-2	32.3 (26)	27.8 (7)	24.3 (19)	18.2 (10)	8.3 (39)	
PPA/TiO_2-3	33.2 (11)	28.3 (4)	25.2 (17)	17.0 (3)	8.4 (65)	
DPA/TiO_2-1	34.1 (25)	28.3 (7)	26.9 (51)	17.7 (1)	9.2 (11)	7.4 (5)
DPA/TiO_2-2	34.4 (20)	28.3 (7)	26.9 (63)	16.8 (3)	9.1 (5)	7.5 (3)
DPA/TiO_2-3	32.4 (29)	28.4 (7)	24.8 (37)	16.4 (3)	9.4 (17)	7.5 (7)

a) Gaussian line shapes are assumed for peaks I to IV, whereas Lorentzian line shapes are assumed for peaks V and VI.

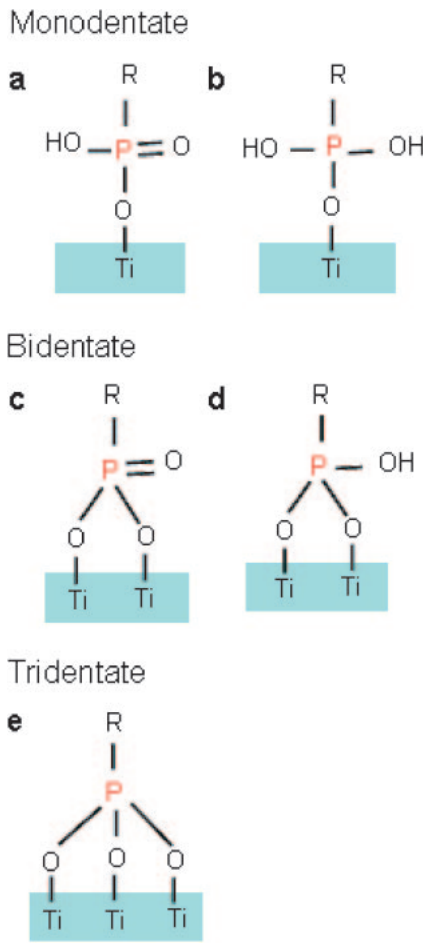

Figure 2. Bonding states of alkylphosphonic acid on TiO_2 surface.

−15 ppm for the first OH and the second OH, respectively, in molecular model systems.[2] The frequency shift was only −3.5 ppm for titania modified by octadecylphosphonic acid, concluding a relatively weak interaction with the TiO_2 surface and perhaps incomplete deprotonation of the phosphonic acid headgroups.[3] The assignment of the observed ^{31}P signal was not established.

The negative frequency shift observed in the present results means that PPA binds on the titania surface. The 8.4-ppm signal is ascribed to the tridentate bonding state **e** from the large frequency shift. In the case of octadecylphosphonic acid binding to TiO_2, ZrO_2, and zirconated silica, a signal was observed at about 7 ppm, which was ascribed to bulk metal alkylphosphonate.[3] On the other hand, the signals between 40 and 10 ppm are ascribed to monodentate and bidentate bonding states, **a** to **d**.

The spectral line shapes in the region between 40 and 10 ppm are similar for the three PPA/TiO_2 samples. The monodentate and bidentate bonding states, **a** to **d**, coexist with some concentrations. On the contrary, the concentration of the tridentate bonding state **e** is largely dependent on the synthetic conditions. Comparison between PPA/TiO_2-2 and -3 samples leads to the conclusion that the tridentate bonding state increases as the conditions become severe, as shown in Figures 1C and 1D.

A broad component around 0 ppm is ascribed to PO_4 species. H_3PO_4 was set at 0 ppm in this work. A small part of PPA is decomposed during the synthesis by breaking a P–C bond.

Figure 3 shows ^{31}P CP/MAS NMR spectra of crystalline DPA and three DPA/TiO_2 samples. Crystalline DPA has two signals at 31.8 and 31.1 ppm, being ascribed to crystallographically inequivalent sites. The DPA/TiO_2 samples have two regions of the signals. One region spreads between 40 and 10 ppm and has a peak at 28.4 ppm, while the other region consists of two signals at 9.4 and 7.5 ppm with relatively narrow line widths. The former is ascribed to monodentate and bidentate bonding states, **a** to **d**, and the latter to tridentate bonding state, **e**. Note that the spectral line shape between 40 and 10 ppm consists of four components ascribed to the bonding states **a** to **d**. This is similar to those of PPA/TiO_2. The spectra are deconvoluted into several components, as before. The deconvolution results between 40 and 10 ppm are drawn in Figure 3, and the parameters of each component are summarized in Table 2. The ^{31}P T_1 value of the 28-ppm signal is 13 s for DPA/TiO_2-1, whereas it is 1300 s for crystalline DPA. The fractions in Table 2 should again be regarded only as a guide, because of the use of CP.

The spectral line shapes in the region between 40 and 10 ppm are similar for the three DPA/TiO_2 samples. The monodentate and bidentate bonding states, **a** to **d**, coexist with some concentrations. On the contrary, the concentration of the tridentate bonding state **e** is largely dependent on the synthetic conditions. Comparison between DPA/TiO_2-2 and -3 samples leads to the conclusion that the tridentate bonding state increases as the conditions become severe, as shown in Figures 3C and 3D. This is the same as PPA/TiO_2. Two signals are observed for the tridentate bonding state **e** in DPA/TiO_2. The fraction of the 9.4-ppm species increases much

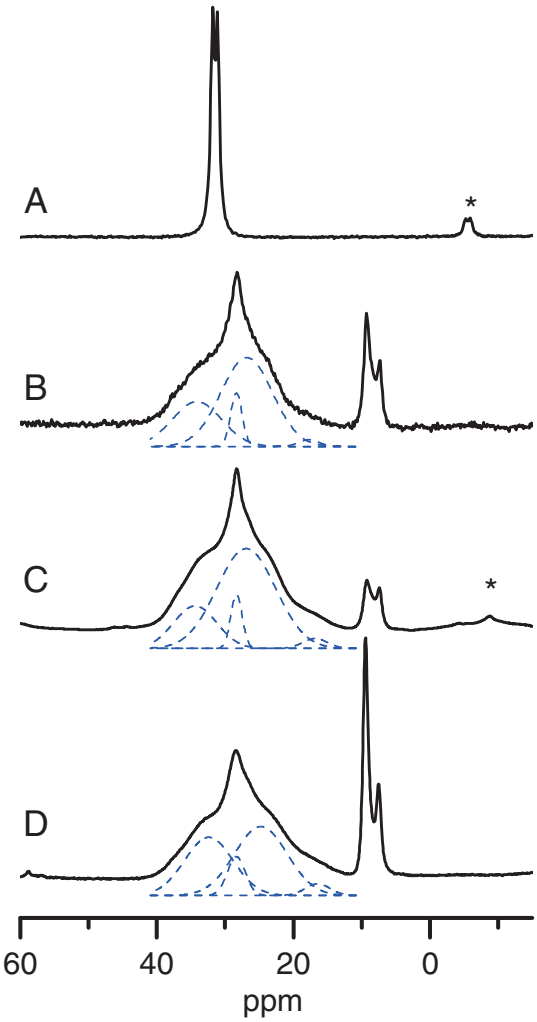

Figure 3. ^{31}P CP/MAS NMR spectra of (A) crystalline DPA, (B) DPA/TiO_2-1, (C) DPA/TiO_2-2, and (D) DPA/TiO_2-3. The spinning rates were (A, C) 6.00, (B) 10.00, and (D) 8.00 kHz. The repetition times were (A) 20 and (B–D) 1 s, and the accumulation numbers were (A) 16, (B) 6225, (C) 50000, and (D) 69850. The mark * indicates spinning sideband. The chain lines show components created by deconvolution in the range between 40 and 10 ppm.

more than that of the 7.5-ppm species with the reaction time. The 9.4-ppm species are more stable than the 7.5-ppm species.

Spin diffusion between ^{1}H spins is useful to study spatial distribution of H-containing species. If ^{1}H spins are concentrated, they have a common spin–lattice relaxation time, because spin diffusion averages the relaxation time. The ^{31}P spectra indicate the presence of monodentate, bidentate, and tridentate bonding states of P. If those P atoms are located in close proximity, ^{1}H spins around P atoms should have a common relaxation time. Thus, we have measured contact time dependence of the signal intensities in ^{31}P CP/MAS NMR spectra. Figure 4 shows the contact time dependence for PPA/TiO_2-3.

The contact time dependence of the signal intensities in ^{31}P CP/MAS NMR spectra is expressed by the following equation in ordinary cases:[18–20]

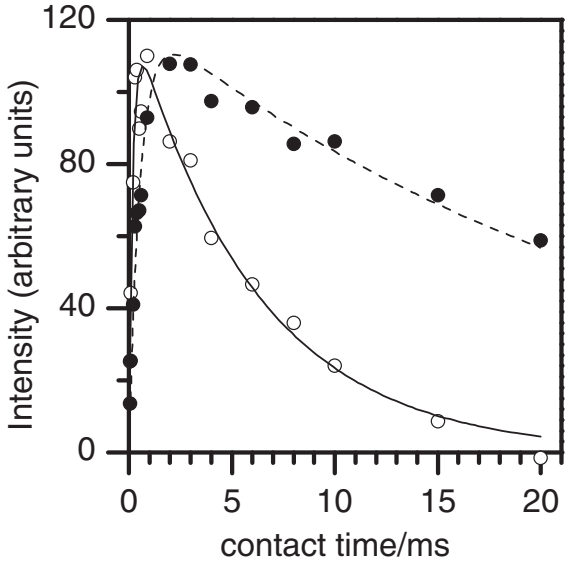

Figure 4. Contact time dependence of the signal intensities in ^{31}P CP/MAS NMR spectra of PPA/TiO_2-3. ○: 28.3 and ●: 8.4 ppm. The spinning rate was 5.00 kHz.

$$M(\tau) = C\frac{\exp\left(-\frac{\tau}{T_{1\rho}(\mathrm{H})}\right) - \exp\left(-\frac{\tau}{T_{\mathrm{HP}}}\right)}{1 - \frac{T_{\mathrm{HP}}}{T_{1\rho}(\mathrm{H})}} \quad (3)$$

where τ is contact time, $M(\tau)$ is signal intensity, $T_{1\rho}$(H) is ^{1}H spin–lattice relaxation time in the rotating frame, and T_{HP} is the cross relaxation time between ^{1}H and ^{31}P. The ^{31}P spin–lattice relaxation time in the rotating frame, $T_{1\rho}$(P), is reasonably assumed to be long enough compared to $T_{1\rho}$(H) in the present samples, and the number of H atoms is large enough compared to that of P atoms. H atoms are contained in PPA and DPA molecules as well as in OH groups on the titania surface. The values of $T_{1\rho}$(H) and T_{HP} were obtained by fitting the obtained results to eq 3, as shown in Figure 4 by lines.

The results of PPA/TiO_2 are summarized in Table 3. The $T_{1\rho}$(H) value of the 8.4-ppm species are longer than those of the other species. This means that the 8.4-ppm species are located at a distant place from other species. In other words, the 8.4-ppm species forms a domain. In the case of DPA/TiO_2 the fitting was not good, and no clear differences were observed between the species.

^{1}H MAS NMR. Figure 5 shows ^{1}H MAS NMR spectra of crystalline PPA and PPA/TiO_2. Crystalline PPA has peaks at 11.2, 1.77, 1.48 (a shoulder peak), and 1.19 ppm, which are ascribed to P–OH, CH_2–P, C–CH_2–C, and CH_3, respectively. A tiny peak is observed at 4.80 ppm, being ascribed to physisorbed H_2O. Liquid water shows a chemical shift of 4.877 ppm.[15]

PPA/TiO_2 has an intense signal at 1.0 ppm, which is assigned to CH_2–P, C–CH_2–C, and CH_3. The line width of each component is broader than that in crystalline PPA, suggesting a distribution of conformation. A small peak is observed at 10 ppm, being ascribed to P–OH. The relative intensity of P–OH is lower than that in PPA, suggesting formation of P–O–Ti bonds. However, the observation of

Table 3. The Values of $T_{1\rho}$(H) and T_{HP} for PPA/TiO_2

Sample	I (33 ppm)		II (28 ppm)		III (25 ppm)		V (8.4 ppm)	
	$T_{1\rho}$(H) /ms	T_{HP} /ms	$T_{1\rho}$(H) /ms	T_{HP} /ms	$T_{1\rho}$(H) /ms	T_{HP} /ms	$T_{1\rho}$(H) /ms	T_{HP} /ms
PPA/TiO_2-1	14	0.2	8	0.2	11	0.2		
PPA/TiO_2-2	14	0.2	7	0.2	15	0.2	22	0.3
PPA/TiO_2-3	11	0.3	6	0.2	11	0.3	26	0.6

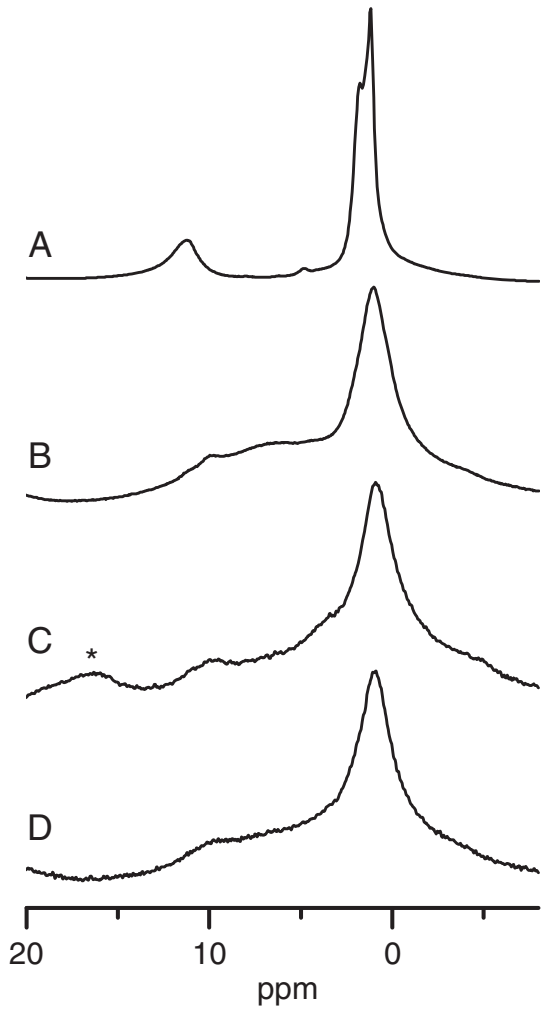

Figure 5. ^{1}H MAS NMR spectra of (A) crystalline PPA, (B) PPA/TiO_2-1, (C) PPA/TiO_2-2, and (D) PPA/TiO_2-3. The spinning rates were (A) 8.06, (B) 8.03, (C) 6.00, and (D) 8.00 kHz. The mark * indicates spinning sideband.

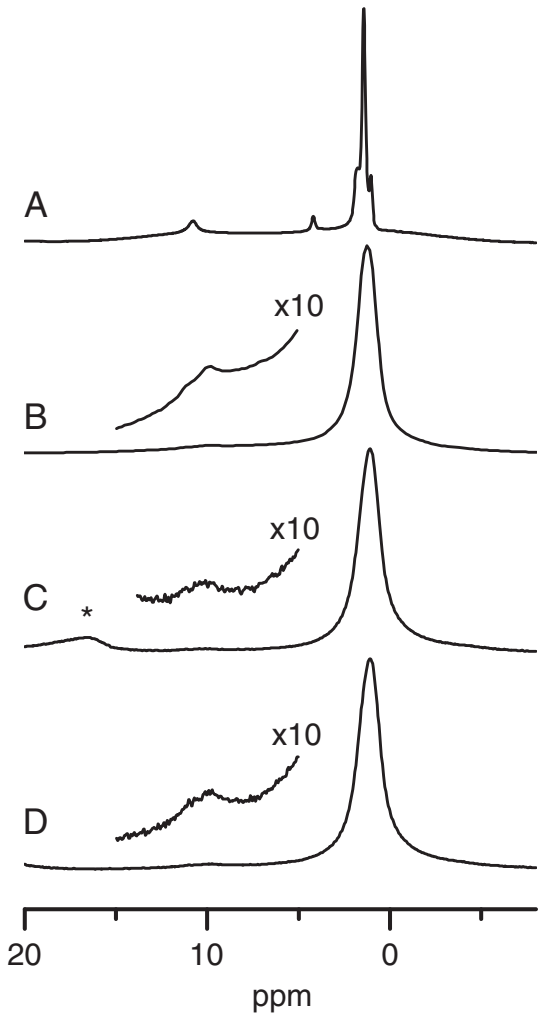

Figure 6. ^{1}H MAS NMR spectra of (A) crystalline DPA (partially hydrated), (B) DPA/TiO_2-1, (C) DPA/TiO_2-2, and (D) DPA/TiO_2-3. The spinning rates were (A, B) 10.00, (C) 6.00, and (D) 8.00 kHz. The mark * indicates spinning sideband.

P–OH demonstrates the presence of the bonding states **a**, **b**, and **d**. A very broad signal is underlying between 10 and 0 ppm, which is ascribed to Ti–OH.

Figure 6 shows ^{1}H MAS NMR spectra of crystalline DPA (partially hydrated) and DPA/TiO_2. The DPA sample shows signals at 10.8, 4.2, 1.8, 1.4, and 1.1 ppm, which are ascribed to P–OH, physisorbed H_2O, CH_2–P, C–CH_2–C, and CH_3, respectively. A very broad hump is underlying, which is ascribed to crystalline DPA. The spinning rate of 10 kHz is not sufficient to suppress the ^{1}H–^{1}H dipolar interaction in crystalline DPA. The observed sharp peaks are due to hydrated DPA. DPA/TiO_2 has an intense signal at 1.3 ppm, which is assigned to CH_2 and CH_3. A very small peak is observed at 10 ppm, being ascribed to P–OH. The relative intensity of P–OH is low compared to that in DPA, suggesting formation of P–O–Ti bonds. The observation of P–OH means the presence of the bonding states **a**, **b**, and **d**. A very broad signal is observed between the above two signals, which is ascribed to Ti–OH.

^{13}C MAS NMR. Conformation of the alkyl chain attached to TiO_2 surface can be probed by ^{13}C NMR. Figure 7 shows ^{13}C CP/MAS NMR spectra of crystalline PPA and PPA/TiO_2. Crystalline PPA has peaks at 29.0, 27.6, 17.2, and 15.3 ppm,

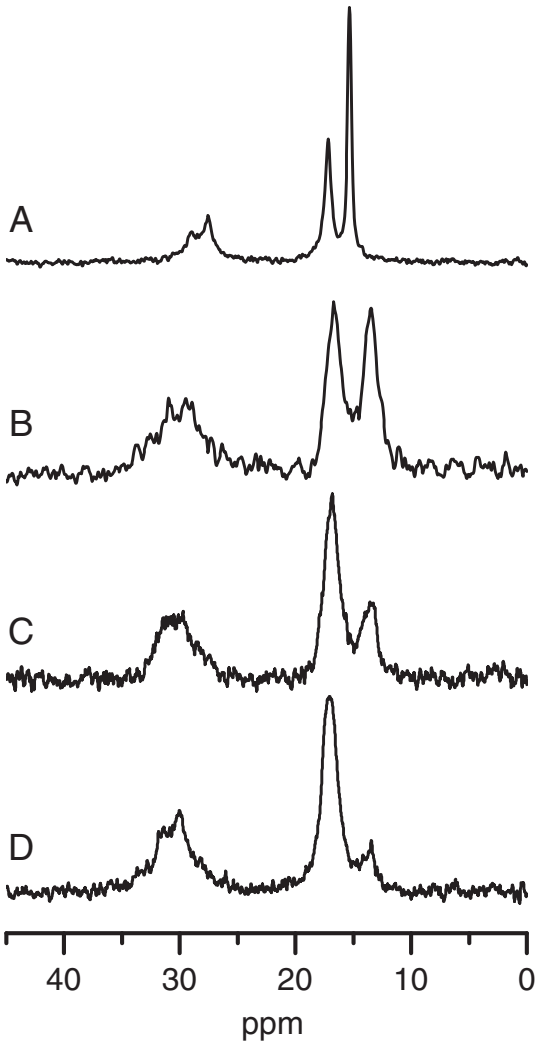

Figure 7. ^{13}C CP/MAS NMR spectra of (A) crystalline PPA, (B) PPA/TiO_2-1, (C) PPA/TiO_2-2, and (D) PPA/TiO_2-3. The spinning rates were (A, B) 4.00, (C) 6.00, and (D) 8.00 kHz.

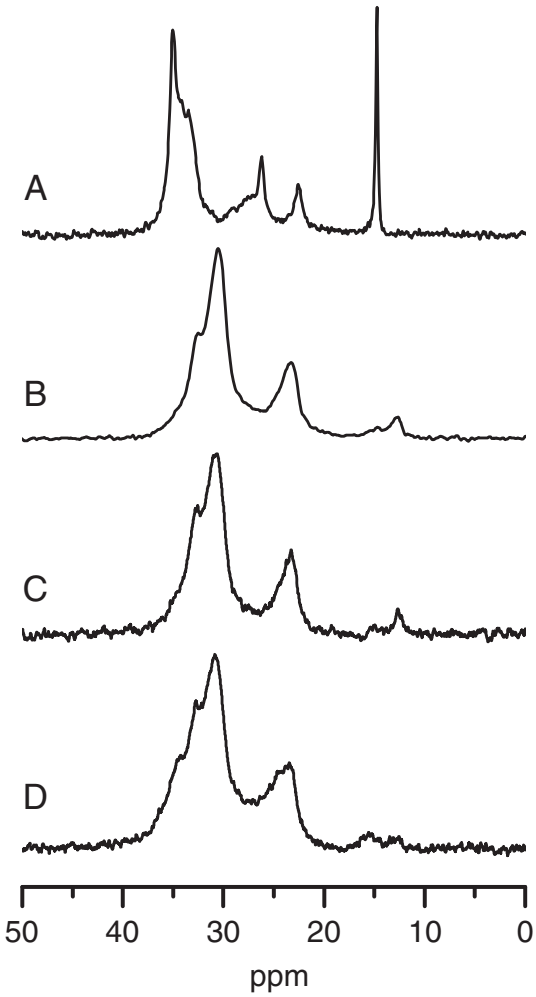

Figure 8. ^{13}C CP/MAS NMR spectra of (A) crystalline DPA, (B) DPA/TiO_2-1, (C) DPA/TiO_2-2, and (D) DPA/TiO_2-3. The spinning rates were (A) 5.00, (B) 4.00, (C) 6.00, and (D) 8.00 kHz.

which are ascribed to CH_2–P, CH_2–P, C–*C*H_2–C, and CH_3, respectively.

PPA/TiO_2 has peaks at ca. 30, 16.7, and 13.5 ppm, which are assigned to CH_2–P, C–*C*H_2–C, and CH_3, respectively. They are shifted by +2, −0.5, and −1.8 ppm, respectively, compared with crystalline PPA. Note that the intensity of the 13.5-ppm signal decreases with respect to that of the 16.7-ppm signal in the order of PPA/TiO_2-1 > PPA/TiO_2-2 > PPA/TiO_2-3. This order is the inverse of the relative intensity of the 8.4-ppm signal in ^{31}P CP/MAS NMR spectra shown in Figure 1. The methyl ^{13}C chemical shift increases when the methyl group is confined in a smaller space.[21–23] In PPA/TiO_2 a portion of methyl signals are shifted to 16.7 ppm by confinement. The 8.4-ppm signal in ^{31}P spectra is closely related to the structure confining methyl group.

Figure 8 shows ^{13}C CP/MAS NMR spectra of crystalline DPA and DPA/TiO_2. Crystalline DPA has peaks at 35.0, 34.2, 33.5, 28, 26.2, 22.6, and 14.7 ppm. The signal at 14.7 ppm is ascribed to methyl groups, and the other signals to CH_2 groups. The signals from 35.0 to 33.5 ppm are assigned to the middle part of methylene chains. The ^{13}C chemical shift of methylene chains depends on the conformation. It is about 33 ppm for the *trans* zigzag structure in a crystalline component, whereas it is about 31 ppm for the methylene carbon in a noncrystalline component undergoing rapid transitions between the *trans* and *gauche* conformations.[24] The values of crystalline DPA indicate that the methylene chain has the *trans* zigzag structure.

The DPA/TiO_2-1 sample shows signals at 32.5, 30.4, 23.3, and 12.5 ppm. The most intense peak at 30.4 ppm suggests that the methylene chain has the *trans–gauche* conformation undergoing rapid transitions between the *trans* and *gauche* conformations. DPA/TiO_2-2 and DPA/TiO_2-3 also have the methylene chain with the *trans–gauche* conformation. DPA/TiO_2-3 has an additional shoulder peak at 35 ppm, suggesting that a part of the methylene chain has the *trans* conformation. Another point to be noted is that a peak is observed at about 15 ppm, being ascribed to methyl groups. A portion of methyl groups are shifted from 12.5 to 15 ppm. Similarly to PPA/TiO_2, a portion of methyl groups are confined in a smaller space. The relative intensity of the 15-ppm signal

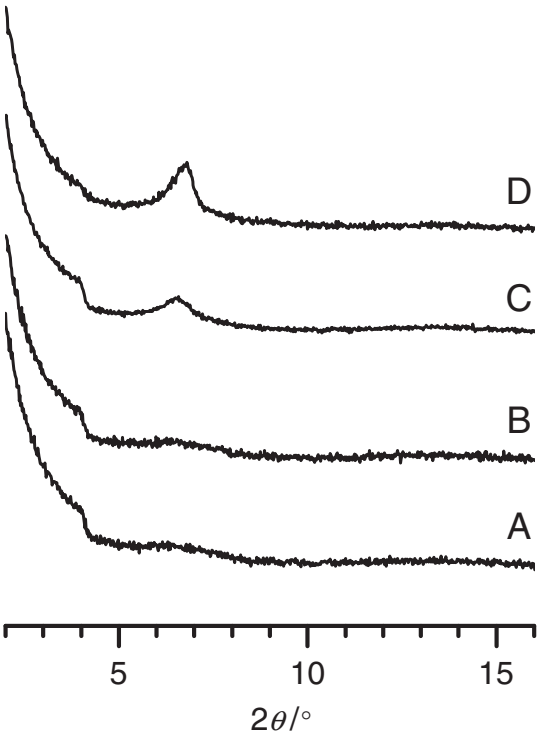

Figure 9. X-ray powder diffraction patterns of (A) TiO_2 nanoparticles, (B) PPA/TiO_2-1, (C) PPA/TiO_2-2, and (D) PPA/TiO_2-3. Only the low angle parts are shown. The step at 4° is an instrumental artifact.

is strongest in PPA/TiO_2-3. The tridentate bonding state of P has the largest concentration in PPA/TiO_2-3 among the three PPA/TiO_2 samples. Thus, the tridentate bonding state of P might be related to a methylene chain with the *trans* conformation and the confined methyl group.

X-ray Diffraction. The production of the tridendate bonding state of P might be related to formation of a layered structure. We then measured X-ray powder diffractions to check the presence of the layered structure. Figure 9 shows X-ray powder diffraction patterns of TiO_2 nanoparticles and PPA/TiO_2. A peak is observed at $2\theta = 6.54°$ in PPA/TiO_2-2 and PPA/TiO_2-3. Those samples have the tridentate bonding state of P. Both the intensity of the diffraction peak and the concentration of the tridentate bonding state of P are larger in PPA/TiO_2-3 than in PPA/TiO_2-2. On the other hand, no peak is observed around $2\theta = 7°$ in PPA/TiO_2-1 which has no tridentate bonding state of P.

Figure 10 shows X-ray powder diffraction patterns of DPA/TiO_2. A peak is observed at $2\theta = 3.2°$ only in DPA/TiO_2-3. On the other hand, no peak is observed at the same region in DPA/TiO_2-1 and DPA/TiO_2-2. DPA/TiO_2-3 has the largest concentration of the tridentate bonding state of P among the three samples.

Thus, the intensities of the above diffraction peaks are closely related to the concentration of the tridentate bonding state of P. The above diffraction peaks strongly support formation of a layered structure, which will be discussed below.

TG-DTA. The amount of attached alkylphosphonic groups was evaluated by thermogravimetric analysis. Figure 11 shows TG curves of PPA/TiO_2-3 and DPA/TiO_2-3. PPA/TiO_2-3

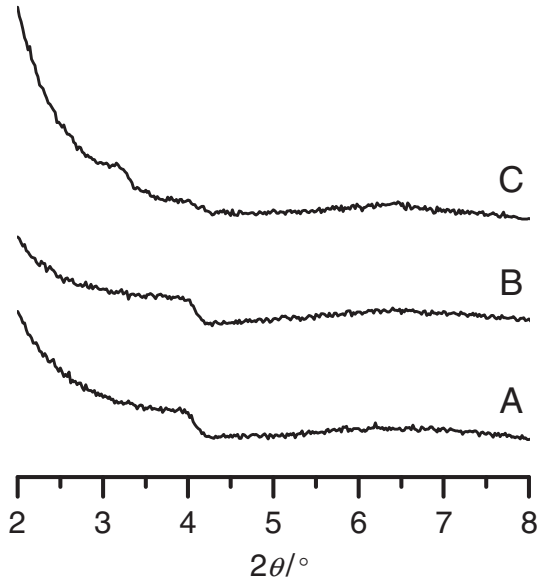

Figure 10. X-ray powder diffraction patterns of (A) DPA/TiO_2-1, (B) DPA/TiO_2-2, and (C) DPA/TiO_2-3. Only the low angle parts are shown. The step at 4° is an instrumental artifact.

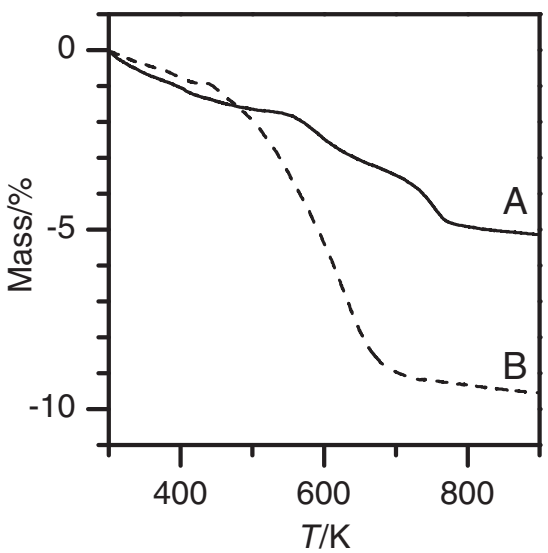

Figure 11. TG curves of (A) PPA/TiO_2-3 and (B) DPA/TiO_2-3.

shows three steps of mass loss. The first step is due to desorption of adsorbed water, and the second and the third steps are decomposition and burning of the organic groups. The second and third steps are accompanied by exothermic peaks. The third step is also observed in PPA/TiO_2-2, but PPA/TiO_2-1 does not have the third step. The tridentate bonding state of P might cause the third step. DPA/TiO_2-3 shows two steps of mass loss. The first step is due to desorption of adsorbed water, and the second step is decomposition and burning of the organic groups. The second step is accompanied by exothermic peaks. DPA/TiO_2-1 and -2 show similar TG curves to DPA/TiO_2-3. The third step is not observed in DPA/TiO_2. The concentration of the tridentate bonding state of P is relatively low, compared to PPA/TiO_2-2 and -3.

Table 4. Results of Thermogravimetric Analysis

Sample name	Mass loss /mass %	Attached molecules /mmol (g-TiO_2)$^{-1}$	Surface coverage /%
PPA/TiO_2-1	2.17	0.66	47
PPA/TiO_2-2	2.89	0.91	64
PPA/TiO_2-3	3.15	1.00	70
DPA/TiO_2-1	7.44	0.63	45
DPA/TiO_2-2	8.09	0.69	49
DPA/TiO_2-3	8.31	0.72	51

Table 5. Tentative Assignments of ^{31}P Signals in Crystalline PPA and PPA/TiO_2

Peak No.	Observed shift /ppm	Case 1[a)]		Case 2[b)]	
		Assignment	Predicted shift /ppm	Assignment	Predicted shift /ppm
	37.4	Crystalline	38	Crystalline	38
I	33	**b**	33	**a**	33
II	28	**a**	28	**b**	28
III	25	**d**	23	**c**	28
IV	18	**c**	18	**d**	23
V	8.4	**e**	13	**e**	18

a) $\Delta_1 = 10$ ppm and $\Delta_2 = 5$ ppm. b) $\Delta_1 = 5$ ppm and $\Delta_2 = 10$ ppm.

The results are summarized in Table 4. The mass of water was excluded in the calculated values. The mass loss was assumed to be caused by the change from Ti–O–P–R to Ti–O–P–$O_{1/2}$, where R is an alkyl group. Only the organic part is burned in the air flow, and P atoms are left as an oxide. Surface coverage was estimated, assuming that the surface area of TiO_2 is 210 m^2, and that one alkylphosphonate molecule occupies 0.24 nm^2.[3] The estimated coverage ranges from 45 to 70%.

Surface Bonding States. PPA and DPA are attached to the surface of titania nanoparticles. The bonding state of the alkylphosphonic acid was probed by ^{31}P NMR. The ^{31}P spectra show four types of bonding states corresponding to the monodentate and bidentate bonding states, **a** to **d**. The tridentate bonding state **e** is concerned with the layered structure, and thus it will be described in the next section.

As listed in Table 2, four components, I to IV, are present between 40 and 10 ppm, which might correspond to bonding states, **a** to **d**. Although an unambiguous assignment of each component is difficult, we wish to propose a tentative assignment, assuming the frequency shift is additive. The frequency shifts caused by reactions (1) and (2) are assumed as $-\Delta_1$ and $-\Delta_2$, respectively. Two cases are possible; case 1 ($\Delta_1 > \Delta_2$) and case 2 ($\Delta_1 < \Delta_2$). The predicted shifts for PPA/TiO_2 are summarized in Table 5. Case 1 can explain the observed shifts fairly well, whereas case 2 cannot explain the tridentate bonding state.

The ^{31}P chemical shifts of components I to IV are similar for PPA/TiO_2 and DPA/TiO_2. The assignment listed in Table 5 (case 1) might be applicable to DPA/TiO_2. The negative frequency shifts caused by reactions (1) and (2) appear to be smaller in DPA/TiO_2 than in PPA/TiO_2, because crystalline DPA shows a smaller chemical shift than crystalline PPA. However, Shimada et al. reported that *n*-alkylphosphonic acid with short *n*-alkyl chains up to 10 CH_2 groups showed a ^{31}P signal at 38–39 ppm in the solid state, while *n*-dodecylphosphonic acid and *n*-octadecylphosphonic acid showed signals at 31 and 33 ppm, respectively.[25] The chemical shifts of 31 to 33 ppm might originate from specific solid state effects in the crystalline compounds.

Although the accuracy of the fraction in Table 2 suffers from the use of CP and the error caused by deconvolution, four components coexist and components I and III are larger than components II and IV. This means that dehydration condensation reaction (1) takes place as well as addition to Lewis acid site (reaction (2)) on TiO_2 nanoparticles. TiO_2 nanoparticle used in this work has the particle size of less than 25 nm and the surface area of 200–220 $m^2\,g^{-1}$. Disorder at the surface might produce a number of Lewis acid sites.

As described in the section of ^{31}P MAS NMR, the assignment of the ^{31}P signals was not established.[2–4,16,17] The present results should be compared with those of hybrid materials of alkylphosphonic acid and TiO_2, because different combinations lead to different results. In the case of TiO_2 modified by octadecylphosphonic acid (ODPA), $HO_2C(CH_2)_nPO_3H_2$ ($n =$ 15 and 11), and dodecylphosphonic acid, a ^{31}P signal was observed at 28 ppm.[3,7,9] A broad component was present at the bottom of the 28-ppm signal,[3,7,9] which was deconvoluted into three components centered at 31.9, 28.0, and 24.6 ppm for the system of dodecylphosphonic acid and TiO_2.[9] No unambiguous assignments were not made. In the present work, we have obtained ^{31}P NMR spectra with good signal/noise ratios, and have demonstrated the presence of four components corresponding to monodentate and bidentate bonding states. We have assigned the four components tentatively, as shown in Table 5.

The ^{1}H NMR spectra demonstrate decrease in P–OH groups due to the dehydration condensation reaction. The observation of P–OH means the presence of the bonding states **a**, **b**, and **d**. The ^{13}C NMR spectra demonstrate that the methylene chain has the *trans–gauche* conformation undergoing rapid transitions between the *trans* and *gauche* conformations.

The surface coverage of the organic modifier is estimated from the mass loss by thermogravimetric analysis. The surface coverage is about 50%, except for PPA/TiO_2-2 and PPA/TiO_2-3 containing considerable amounts of the layered structure.

Formation of Layered Structure. Prolonged heating of the mixed solution of the reactants produces layered organophosphonates, as described below. The diffraction peaks at $2\theta = 6.54°$ in PPA/TiO_2-2 and -3, and $2\theta = 3.2°$ in DPA/TiO_2-3 strongly support formation of a layered structure. Those diffraction peaks are indexed as (001) if the layer is accumulated in the *c* direction. The interlayer distance can be estimated from the diffraction angle. A number of layered organophosphonates have been prepared by combining solutions of soluble metal salts and alkyl- or arylphosphonic acids.[26–28] The interlayer distances depend on the length of alkyl chain, which are 1.35 and 2.76 nm for PPA/TiO_2 and DPA/TiO_2, respectively. The increment of the interlayer distance per one carbon atom is 0.201 nm, which is larger than the increment for all-*trans n*-alkyl chain (0.127 nm)[25] and smaller than the doubled value (0.254 nm). This means bilayer

arrangement of the *n*-alkyl chains in the interlayer space. The ^{13}C NMR results suggest all-*trans* conformation of *n*-alkyl chains, and the molecular axis of the *n*-alkyl chains is tilted at 52° from the layer plane. The ^{13}C NMR results suggest that the methyl group is confined in a small space. The alkyl chains are sandwiched between titanium oxide layers, and then the methyl groups are surrounded by alkyl chains.

The ^{31}P NMR results demonstrate that the tridentate bonding state **e** is formed in the layered structure. The ^{1}H $T_{1\rho}$ values suggest that the tridentate bonding state **e** forms a domain and is located at a distant place from other bonding states.

PPA/TiO_2-2 and PPA/TiO_2-3 show the third step of mass loss in the TG curve. The two samples contain large amounts of the layered substances. The layered substances might be a little bit refractory, because organic groups are covered by inorganic plates. PPA/TiO_2-2 and PPA/TiO_2-3 appear to have a larger surface coverage than the other samples. This is due to formation of the layered structure. The alkyl chains are crowded in the interlayer space.

Conclusion

We have modified the surface of TiO_2 nanoparticles by propylphosphonic acid (PPA) and decylphosphonic acid (DPA), and have characterized the surface layer of titania nanoparticles by means of high-resolution solid-state NMR of ^{31}P, ^{1}H, and ^{13}C, X-ray powder diffraction, and themogravimetric analysis. The following conclusions are obtained:

(1) The bonding state of the alkylphosphonic acid was probed by ^{31}P NMR. The ^{31}P spectra show four types of bonding states corresponding to the monodentate and bidentate bonding states, **a** to **d**. The tridentate bonding state **e** is formed by prolonged heating of the mixed solution of the reactants. Dehydration condensation reaction takes place as well as addition to Lewis acid site on TiO_2 nanoparticles. The ^{1}H NMR spectra demonstrate decrease in P–OH groups due to the dehydration condensation reaction.

(2) Layered titanium alkylphosphonate is formed by prolonged heating. X-ray powder diffraction patterns indicate the layered structure, and the interlayer distance suggests bilayer arrangement of the *n*-alkyl chains in the interlayer space. The ^{13}C NMR results suggest all-*trans* conformation of *n*-alkyl chains, and the methyl group is confined in a small space. The molecular axis of the *n*-alkyl chains is tilted from the perpendicular of the layer plane.

(3) The surface coverage of the organic modifier is estimated from the mass loss by thermogravimetric analysis. The surface coverage is about 50%, except for the samples containing considerable amounts of the layered structure.

A part of this work was financially supported by New Energy and Industrial Technology Development Organization (NEDO) of Japan.

References

1 A. Ulman, *Chem. Rev.* **1996**, *96*, 1533.
2 I. Lukeš, M. Borbaruah, L. D. Quin, *J. Am. Chem. Soc.* **1994**, *116*, 1737.
3 W. Gao, L. Dickinson, C. Grozinger, F. G. Morin, L. Reven, *Langmuir* **1996**, *12*, 6429.
4 G. Guerrero, P. H. Mutin, A. Vioux, *Chem. Mater.* **2001**, *13*, 4367.
5 J. Randon, P. Blanc, R. Paterson, *J. Membr. Sci.* **1995**, *98*, 119.
6 T. Arita, J. Yoo, T. Adschiri, *J. Phys. Chem. C* **2011**, *115*, 3899.
7 S. Pawsey, K. Yach, L. Reven, *Langmuir* **2002**, *18*, 5205.
8 V. Lafond, C. Gervais, J. Maquet, D. Prochnow, F. Babonneau, P. H. Mutin, *Chem. Mater.* **2003**, *15*, 4098.
9 F. Brodard-Severac, G. Guerrero, J. Maquet, P. Florian, C. Gervais, P. H. Mutin, *Chem. Mater.* **2008**, *20*, 5191.
10 S. Pawsey, M. McCormick, S. De Paul, R. Graf, Y. S. Lee, L. Reven, H. W. Spiess, *J. Am. Chem. Soc.* **2003**, *125*, 4174.
11 W. Gao, L. Dickinson, C. Grozinger, F. G. Morin, L. Reven, *Langmuir* **1997**, *13*, 115.
12 D. A. Torchia, *J. Magn. Reson.* **1978**, *30*, 613.
13 S. Hayashi, K. Hayamizu, *Bull. Chem. Soc. Jpn.* **1989**, *62*, 2429.
14 S. Hayashi, M. Mizuno, *Solid State Commun.* **2004**, *132*, 443.
15 S. Hayashi, K. Hayamizu, *Bull. Chem. Soc. Jpn.* **1991**, *64*, 685.
16 W. Gao, L. Reven, *Langmuir* **1995**, *11*, 1860.
17 G. Guerrero, P. H. Mutin, A. Vioux, *Chem. Mater.* **2000**, *12*, 1268.
18 M. Mehring, *Principles of High Resolution NMR in Solids*, Springer-Verlag, **1983**.
19 S. Ando, R. K. Harris, S. A. Reinsberg, *J. Magn. Reson.* **1999**, *141*, 91.
20 W. Kolodziejski, J. Klinowski, *Chem. Rev.* **2002**, *102*, 613.
21 S. Hayashi, K. Suzuki, K. Hayamizu, *J. Chem. Soc., Faraday Trans. 1* **1989**, *85*, 2973.
22 S. Hayashi, E. Akiba, *Chem. Phys. Lett.* **1994**, *226*, 495.
23 S. Hayashi, *J. Phys. Chem.* **1995**, *99*, 7120.
24 I. Ando, T. Yamanobe, S. Akiyama, T. Komoto, H. Saito, T. Fujito, K. Deguchi, M. Imanari, *Solid State Commun.* **1987**, *62*, 785.
25 A. Shimada, Y. Yoneyama, S. Tahara, P. H. Mutin, Y. Sugahara, *Chem. Mater.* **2009**, *21*, 4155.
26 G. Cao, H. Lee, V. M. Lynch, T. E. Mallouk, *Solid State Ionics* **1988**, *26*, 63.
27 G. Cao, H. Lee, V. M. Lynch, T. E. Mallouk, *Inorg. Chem.* **1988**, *27*, 2781.
28 G. Cao, H.-G. Hong, T. E. Mallouk, *Acc. Chem. Res.* **1992**, *25*, 420.